Predictions of pressure-induced structural transition, mechanical and thermodynamic properties of α- and β-Si_3N_4 ceramics: *ab initio* and quasi-harmonic Debye modeling*

Yu Ben-Hai(余本海) and Chen Dong(陈 东)†

College of Physics and Electronic Engineering, Xinyang Normal University, Xinyang 464000, *China*

(Received 24 October 2011; revised manuscript received 3 December 2011)

The plane-wave pseudo-potential method within the framework of *ab initio* technique is used to investigate the structural and elastic properties of α- and β-Si_3N_4. The ground-state parameters accord quite well with the experimental data. Our calculation reveals that α-Si_3N_4 can retain its stability to at least 40 GPa when compressed at 300 K. The α → β phase transformation would not occur in a pressure range of 0–40 GPa and a temperature range of 0–300 K. Actually, the α → β transition occurs at 1600 K and 7.98 GPa. For α- and β-Si_3N_4, the *c* axes are slightly more incompressible than the *a* axes. We conclude that β-Si_3N_4 is a hard material and ductile in nature. On the other hand, β-Si_3N_4 is also found to be an ionic material and can retain its mechanical stability in a pressure range of 0–10 GPa. Besides, the thermodynamic properties such as entropy, heat capacity, and Debye temperature of α- and β-Si_3N_4 are determined at various temperatures and pressures. Significant features in these properties are observed at high temperature. The calculated results are in good agreement with available experimental data and previous theoretical values. Many fundamental solid-state properties are reported at high pressure and high temperature. Therefore, our results may provide useful information for theoretical and experimental investigations of the Si_3N_4 polymorphs.

Keywords: *ab initio*, elastic constants, phase transition, Poisson ratio

PACS: 05.70.Fh, 21.60.De, 62.20.dq **DOI:** 10.1088/1674-1056/21/6/060508

1. Introduction

Silicon nitride (Si_3N_4), which belongs to the family of group IV nitrides, is an important technical material as a ceramic and as a dielectric insulator.[1] Due to its high hardness and strength, high decomposition temperature, low compressibility, good corrosion resistance, wear resistance, and thermal shock resistance, Si_3N_4 is used as a high-temperature structural material for cutting tools, engineering dies, antifriction bearings, and gas engines.[2] Its low density, tunable electrical conductivity, good creep resistance, and fracture toughness lead to numerous applications in nuclear industry and space project.[3] There are two well-known crystalline phases of silicon nitride: α- and β-Si_3N_4, both have hexagonal structures. β-Si_3N_4 is generally considered to be more stable than α-Si_3N_4 under ambient conditions. About 13 years ago, the third polymorph (spinel γ-Si_3N_4) was synthesized by Zerr *et al.*[4]

Wang *et al.*[5] have investigated the bulk moduli and the thermodynamic properties of α-, β-, and γ-Si_3N_4 by using the analytic mean-field method. Chen *et al.*[6] have computed the phonon density of states and heat capacity for β-Si_3N_4 through lattice dynamics. Using the same method, Kuwabara *et al.*[7] have determined the phonon dispersion curves, phonon densities of states (DOSs), bulk moduli, thermal expansion coefficients, and heat capacities of α-, β-, and γ-Si_3N_4. Some thermodynamic properties, such as heat capacities, entropies, free energies, phonon DOSs, and phonon dispersion curves for α- and β-Si_3N_4, are also given in Refs. [8] and [9]. Nevertheless, in these above-mentioned papers the properties are often obtained at zero pressure and some important thermodynamic quantities are missing. Dodd *et al.*[10] have measured the cell volumes, shear moduli, and Young's moduli of β-Si_3N_4 at different pressures and temperatures. In their work the temperature is limited to 300 K and some important elastic moduli (for exam-

*Project supported by the National Natural Science Foundation of China (Grant Nos. 11105115 and 11005088) and the Project of Basic and Advanced Technology of Henan Province, China (Grant No. 112300410021).

†Corresponding author. E-mail: chchendong2010@163.com

© 2012 Chinese Physical Society and IOP Publishing Ltd

ple: bulk moduli and elastic constants) are missing. Moreover, the structural properties, electronic structures, and optical properties of the Si_3N_4 polymorphs are discussed in Refs. [2], [11], and [12].

The slightly less dense α-Si_3N_4 undergoes an irreversible first-order phase transformation into the β phase at high temperature.[11,13] The polymorphic α → β phase transition in Si_3N_4 has a considerable effect on the consolidation and grain-structure formation as well as on the strength of the Si_3N_4-based ceramics.[14] As given in Ref. [15], the α → β phase transition occurs at 3 GPa–6 GPa. The transition pressure between β- and γ-Si_3N_4 is around 12.5 GPa,[16] which indicates that the transition pressure between α- and β-Si_3N_4 is less than 12.5 GPa. Through the X-ray diffraction experiment, Kruger *et al.*[17] have found that α-Si_3N_4 can retain its stability to 48 GPa when compressed statically at 295 K. The X-ray diffraction also shows that the α → β phase transition begins at 1573 K ($P = 7.7$ GPa) and ends at 2373 K.[14] The information on the α → β phase transition is highly conflicting and the transition character is still unclear now.[14,18] Very recently, Xu *et al.*[2] have investigated the α → γ, β → γ, and β → δ phase transition characters for the Si_3N_4 polymorphs, where δ-Si_3N_4 is an unknown new phase.[4] Some thermodynamic properties like thermal expansion coefficient and Grüneisen parameter are investigated in their work. Nevertheless, the pressure effects on the thermodynamic quantities are not considered and the α → β phase transition process is missing. To the author's knowledge, previous investigations often concentrated on β-Si_3N_4 and the newly discovered γ-Si_3N_4. Little attention has been paid to α-Si_3N_4 especially at high temperature. The understanding of some fundamental properties such as bulk modulus, entropy, heat capacity, and Debye temperature of α-Si_3N_4 is far from complete. We believe that the theoretical study on the thermodynamic properties of α- and β-Si_3N_4 is very important for applications.

The aim of this paper is to highlight the phase transition characters between α- and β-Si_3N_4. The second goal of this paper is to determine the high-pressure and high-temperature elastic properties and thermodynamic properties of α- and β-Si_3N_4. In Section 2, the computational details are presented. Then, the computed results of lattice structures, elastic moduli, thermal properties, and phase transition characters are discussed in Section 3. Finally, conclusions are drawn from the present study in Section 4.

2. Computational method

Under ambient conditions, β-Si_3N_4 (phenacite-type) has a hexagonal structure with two Si_3N_4 molecular units (14 atoms) per unit cell. α-Si_3N_4 (nierite) has a unit cell twice as large as that of β-Si_3N_4 and each unit cell contains atoms twice as many as atoms per unit cell of β-Si_3N_4. α-Si_3N_4 crystallizes into a trigonal structure, with space gourp $P3_1c$.[7] Silicon atoms occupy the 6*c* (1/12, 1/2, 3/4) and 6*c* (1/4, 1/6, 1/2) Wyckoff sites. Nitrogen atoms occupy 6*c* (2/3, 2/3, 1/2), 6*c* (1/3, 1/3, 3/4), 2*b* (1/3, 2/3, 3/4), and 2*a* (0, 0, 1/2) positions.[19] For bulk β-Si_3N_4, the $P6_3/m$ structure is used in our calculation.[20,21] Different atoms occupy several 6h sites, namely N (1/3, 2/3, 1/4), N (0.321, 0.025, 0.25), and Si (0.1740, 0.7659, 0.25) positions.[20−22] The α-phase is usually recognized as being meta-stable relative to the β-phase.[17,23,24] The fundamental structures in α- and β-Si_3N_4 are both the corner-linked SiN_4 tetrahedra, linked in such a way that the NSi_3 unit is approximately planar.[9]

The ground-state structures of α- and β-Si_3N_4 are optimized in the framework of the *ab initio* method based on the Kohn–Sham equation.[25] The self-consistent total energy calculations are performed with the plane-wave pseudo-potential (PW-PP) method.[26] The generalized gradient approximation (GGA) of Perdew–Burke–Ernzerhof[27] is used for the exchange–correlation functional. Convergence tests guided the choice of 500 eV for the cutoff energy. Pseudo-atomic calculations are performed for Si-$3s^2 3p^2$ and N-$2s^2 2p^3$, and all the pseudo-potentials are non-local. The *k*-point meshes of the Brillouin zone, based on the Monkhorst–Pack scheme,[28] are 4×4×7 for α-Si_3N_4 and 4×4×12 for β-Si_3N_4, respectively. Equilibrium structures of α- and β-Si_3N_4 are optimized until the total energies are converged to at least 10^{-6} eV/atom and the Hellman–Feynman force becomes smaller than 5×10^{-2} eV/nm.

According to the standard thermodynamics, if a system is held at finite temperature then the Gibbs free energy G can be expressed as

$$G(V;P,T) = E(V) + PV - TS, \qquad (1)$$

where $E(V)$ is the total energy, V the cell volume and S the entropy of the system. Since the experimental determination of thermodynamic properties often takes place at a finite temperature and therefore the vibrational effects should be considered. So we choose the vibrational Debye-like method (QHD

method)[29] and according to this model the non-equilibrium Gibbs free energy $G^*(V;P,T)$ can be written as

$$G^*(V;P,T) = E(V) + PV + A_{\rm vib}(T,\theta_D(V)), \quad (2)$$

where PV corresponds to the constant hydrostatic pressure condition and $A_{\rm vib}$ is the vibrational Helmholtz free energy. A series of standard thermodynamic relations can be determined by fitting the calculated E–V data to the Birch–Murnaghan equation of state (EOS)[30]

$$P = 3B_0 f_E(1+2f_E)^{5/2}\left[1+\frac{3}{2}(B'-4)f_E + \frac{3}{2}\left(B_0B'' + (B'-4)(B'-3) + \frac{35}{9}\right)f_E^2\right], \quad (3)$$

where $f_E = [(V_0/V)^{2/3}-1]/2$. Then, some thermodynamic properties such as heat capacity C_v, entropy S, and Debye temperature $\theta_{\rm D}$ can be determined by

$$C_v = 3nk_{\rm B}\left[4D(\theta_{\rm D}/T) - \frac{3\theta_{\rm D}/T}{{\rm e}^{\theta_{\rm D}/T}-1}\right], \quad (4)$$

$$S = nk_{\rm B}\left[4D(\theta_{\rm D}/T) - 3\ln(1-{\rm e}^{-\theta_{\rm D}/T})\right], \quad (5)$$

$$\theta_{\rm D} = \frac{h}{2\pi}(6\pi^2V^{1/2}n)^{1/3}f(\sigma)\sqrt{\frac{B_S}{k_{\rm B}^2M}}, \quad (6)$$

where V, M, n, B_S, $f(\sigma)$, and $k_{\rm B}$ are the primitive cell volume, the molar mass, the number of atoms per unit cell, the adiabatic bulk modulus, a scaling function that depends on Poisson ratio σ of the isotropic crystal, and the Boltzmann's constant, respectively, and $D(\theta_{\rm D}/T)$ represents the Debye integral. A detailed expression of the QHD method can be found in Ref. [29] and references therein.

3. Results and discussion

3.1. Equilibrium crystal structure

As a first step, Si_3N_4 are optimized under pressure and under no pressure, and the results are shown in Fig. 1. At 0 GPa, the calculated equilibrium lattice constants are $a = 0.7781$ nm and $c = 0.5641$ nm for α-Si_3N_4. From Fig. 1(a), we can see that the lattice parameters a and c decrease with applied pressure increasing and the relationships between these parameters and pressures are all linear. The calculated lattice constants are a little larger than the experimental values for α- and β-Si_3N_4. This is due mainly to the fact that GGA usually overestimates lattice constants. The maximum relative error is only 0.47%, which is within the general accuracy of *ab initio* methods using GGA (usually 1%–2%). Our results and the theoretical values ($a = 0.7757$ nm, $c = 0.5623$ nm;[17] $a = 0.7754$ nm, $c = 0.5630$ nm;[31] $a = 0.7761$ nm, $c = 0.5628$ nm;[9] $a = 0.7718$ nm, $c = 0.5591$ nm;[32] $a = 0.7792$ nm, $c = 0.5614$ nm[22]) and the experimental data ($a = 0.7755$ nm, $c = 0.5621$ nm;[11] $a = 0.7766$ nm, $c = 0.5615$ nm[33]) for α-Si_3N_4 are in excellent agreement. For β-Si_3N_4, the theoretical values ($a = 0.7593$ nm, $c = 0.2921$ nm;[31] $a = 0.7533$ nm, $c = 0.2934$ nm;[9] $a = 0.7622$ nm, $c = 0.2910$ nm;[22] $a = 0.7595$ nm, $c = 0.2902$ nm[32]) and the experimental data ($a = 0.7607$ nm, $c = 0.2907$ nm;[11] $a = 0.7607$ nm, $c = 0.2911$ nm[34]) are reliable. The obtained lattice parameters are also very close to the reported values of β-Si_3N_4. The computed lattice parameters and other available results are also in good agreement, indicating that our calculations are valid and reliable. To the best of our knowledge, in the case of high pressure no previous experimental and theoretical results are available to compare with our data.

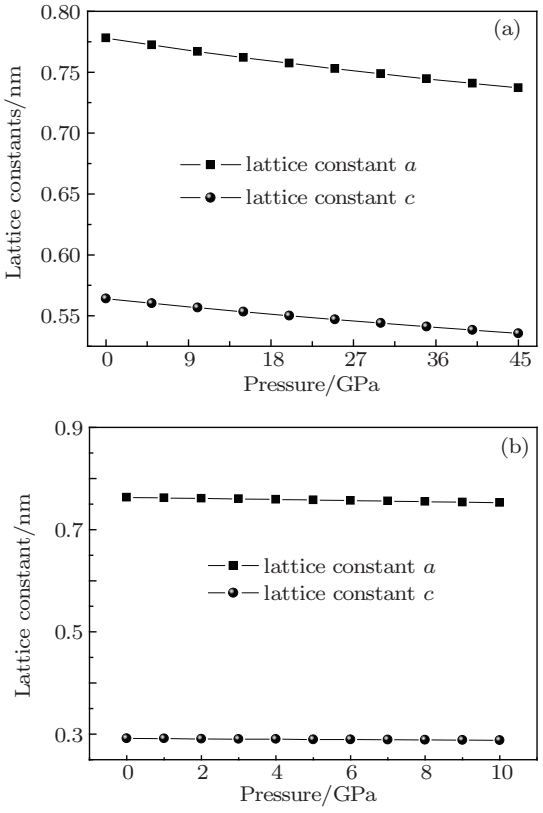


Fig. 1. Structural parameters of α-Si_3N_4 (a) and β-Si_3N_4 (b) at different pressures.

According to the Voigt–Reuss–Hill approximations,[35] the polycrystalline bulk modulus B_H, shear modulus G_H, Young's modulus E, Poisson ratio σ, and compressibility K can be obtained respectively

by

$$B_H = \frac{B_V + B_R}{2}, \quad G_H = \frac{G_V + G_R}{2}, \tag{7}$$

$$E = \frac{9B_H G_H}{3B_H + G_H}, \quad \sigma = \frac{3B_H - 2G_H}{2(3B_H + G_H)}, \tag{8}$$

$$K = \frac{(C_{11} + C_{12})C_{33} - 2C_{13}^2}{C_{11} + C_{12} + 2C_{33} - 4C_{13}}. \tag{9}$$

The calculated results for β-Si_3N_4 are shown in Fig. 2. Unfortunately, we cannot calculate the elastic constants of α-Si_3N_4.

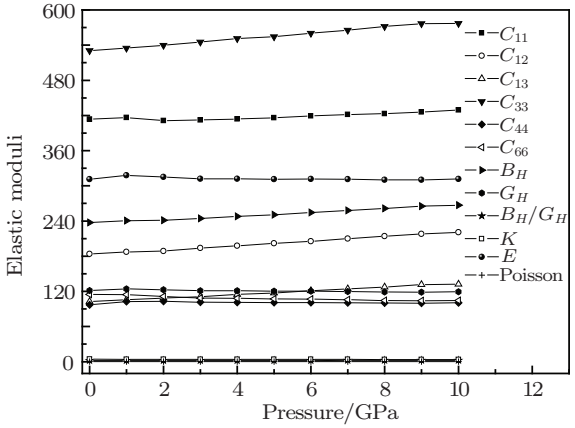


Fig. 2. Elastic constants C_{ij} (GPa), polycrystalline bulk modulus B_H (GPa), shear modulus G_H (GPa), compressibility K (10^{-3}/GPa), Young's modulus E (GPa), compressibility K (10^{-3}/GPa), B_H/G_H ratio, and Poisson ratio σ for β-Si_3N_4.

As is well known, the hardness and strength of solids are related to their elastic moduli. From Figs. 1 and 2, one can see that a decrease in lattice constant leads to an enhancement in bulk modulus. All the elastic constant C_{ij} (except C_{44} and C_{66}) and elastic moduli (except G_H, B_H/G_H, K, E, and σ) increase monotonically when the pressure is enhanced, but the slopes of their increase are different from each other. C_{66}, K, and σ decrease with applied pressure increasing while E, C_{44}, and G_H first increase, and then gradually decrease with pressure increasing. β-Si_3N_4 is almost incompressible at high pressures. According to the Pugh's criterion,[36] a material is ductile if the B/G ratio is larger than 1.75. Our calculations have given the B/G ratios of 1.954–2.238 at different pressures, suggesting a ductile behaviour in β-Si_3N_4.[37] The ductility of β-Si_3N_4 increases with pressure increasing. On the other hand, it is generally believed that the values of Poisson ratio smaller than 0.1 are associated with covalent compound, whereas ionic materials have typical values close to 0.25.[38] For covalent and ionic solids, the typical relations between bulk and shear modulus are $G/B \approx 1.1$ and $G/B \approx 0.6$, respectively.[39] The G/B ratio and the Poisson ratio vary from 0.516 to 0.447 and from 0.281 to 0.306 in pressure range 0–10 GPa, respectively. These results imply that the chemical boding in β-Si_3N_4 is more ionic than covalent, which is in agreement with the results given in Ref. [40]. Moreover, the Born's mechanical stability criteria[41] for hexagonal lattice are

$$C_{11} > |C_{12}|, \tag{10}$$

$$(C_{11} + C_{12})C_{33} - 2C_{13}^2 > 0, \tag{11}$$

$$C_{44} > 0, \quad C_{66} > 0. \tag{12}$$

The elastic constants shown in Fig. 2 satisfy all these inequalities. Therefore, β-Si_3N_4 can retain its mechanical stability in pressure range 0–10 GPa.

The experimental data (C_{11} = 343 GPa–433 GPa, C_{12} = 136 GPa–195 GPa, C_{13} = 120 GPa–127 GPa, C_{33} = 574 GPa–600 GPa, C_{44} = 108 GPa–124 GPa, $C_{66} =\sim$ 119 GPa)[42,43] and the theoretical values (C_{11} = 409.3 GPa, C_{12} = 271.2 GPa, C_{13} = 200.6 GPa, C_{33} = 603.6 GPa, C_{44} = 108.0 GPa, C_{66} = 69.0 GPa),[9] (C_{11} = 447.5 GPa, C_{12} = 214.6 GPa, C_{13} = 165.1 GPa, C_{33} = 580.2 GPa, C_{44} = 115.0 GPa, C_{66} = 116.5 GPa)[8] are used to compare with our results. Using molecular dynamics, Hirosaki *et al.*[32] have calculated the elastic constants of β-Si_3N_4. Their values are C_{11} = 591 GPa, C_{12} = 182 GPa, C_{13} = 162 GPa, C_{33} = 690 GPa, C_{44} = 189 GPa, and C_{66} = 205 GPa. The experimentally determined elastic constants are widely scattered, because such measurements would require the availability of Si_3N_4 single crystal samples of reasonable size. Generally speaking, our calculated elastic constants are in agreement with these results. Consider the fact that GGA usually underestimate bulk modulus, the experimentally measured elastic moduli (B = 233 GPa, G = 123 GPa,[44] B = 249 GPa,[45] B = 259 GPa,[43] and B = 238 GPa, E = 306 GPa, σ = 0.285[10]) and the theoretical values (B = 262.1 GPa,[31] B = 234 GPa,[46] B = 232.7 GPa–266 GPa[2]) also proven the validity of our calculations.

3.2. Phase transition

Firstly, the pressure dependence of enthalpy difference H_β–H_α is plotted in Fig. 3(a). It can be seen that the enthalpy difference decreases initially with

applied pressure increasing and then increases at high pressure ($P > 25$ GPa). $H_\beta < H_\alpha$ holds true in the whole pressure range 0–40 GPa, which implies that β-Si_3N_4 is more stable than α-Si_3N_4. Clearly the maximum enthalpy difference −0.062 eV corresponds to $P = 25$ GPa. Nevertheless, H_β–H_α is so small that we are not sure whether the pressure-induced phase transition will occur during the increase of pressure. Then, the pressure dependence of total energy difference E_β–E_α is calculated and displayed in Fig. 3(b). When $P < 10$ GPa, the energy difference E_β–E_α decreases slowly with applied pressure increasing. When $P > 10$ GPa, E_β–E_α decreases dramatically as P increases. In the whole pressure range of 0–40 GPa, the energy differences are negative, which also implies that β-Si_3N_4 is more stable than α-Si_3N_4. Finally, in order to obtain a deep insight into the phase stability of Si_3N_4, we carry out the calculations of the Gibbs free energy for the involved polymorphs. Since the PW–PP method is unable to obtain the Gibbs free energy at non-zero temperature, the QHD method is used to calculate the Gibbs free energy and the results are drawn in Fig. 3(c).

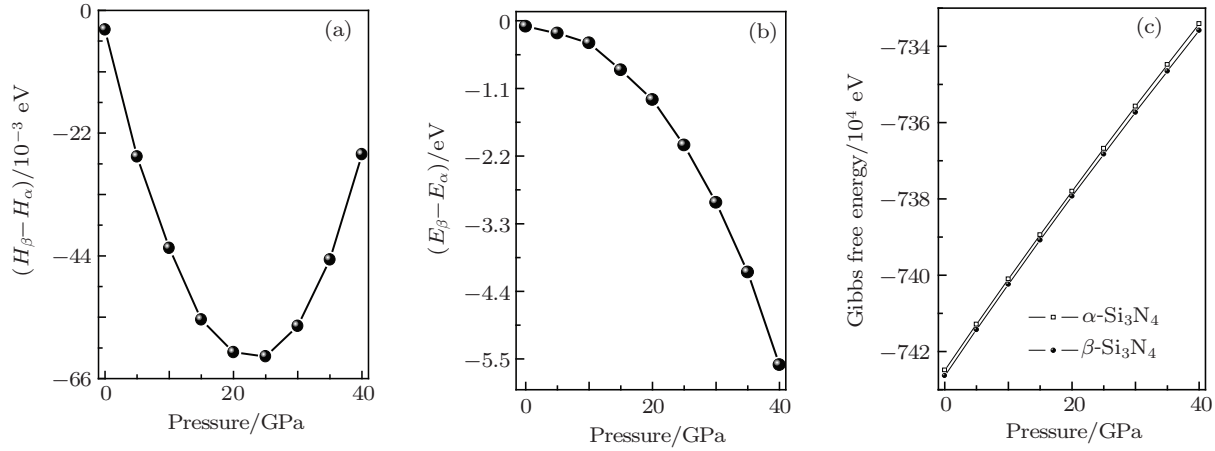


Fig. 3. Pressure dependences of enthalpy difference H_β–H_α obtained by the plane-wave pseudo-potential method (a); pressure versus total energy difference E_β–E_α at 0 K (b); Gibbs free energy variations versus applied pressure for α- and β-Si_3N_4 (QHD) at 300 K.

Figure 3(c) shows the changes of Gibbs free energy with the increase of pressure for α- and β-Si_3N_4. It is obviously seen that the Gibbs free energy smoothly increases with pressure increasing. The Gibbs free energy of β-Si_3N_4 is always smaller than that of α-Si_3N_4 in the pressure range 0–40 GPa, which is in agreement with the results shown in Ref. [2]. Thus, the phase transition will not occur during the increase of pressure. β-Si_3N_4 is more stable under pressure. This means, consistently with the experimental observation,[23] that β-Si_3N_4 is more energy favourable than α-Si_3N_4. Pressure may distort the tetrahedral structure in α-Si_3N_4 toward a more β-like tetrahedral structure, without changing the long-range order of the α-Si_3N_4 crystal.[17] At 0 K, the Gibbs free energy curves are similar to the curves shown in Fig. 3(c), so these 0 K curves are not given there.

Summarizing, the phase transition between α- and β-Si_3N_4 will not occur in temperature range 0–300 K and pressure range 0–40 GPa. Although β-Si_3N_4 transforms into γ-Si_3N_4 at high temperature and high pressure,[2] the β phase is stable up to at least 40 GPa (at 300 K). Through the X-ray diffraction experiment, Kruger *et al.*[17] have found that the α-Si_3N_4 crystal is meta-stable to at least 48 GPa when compressed statically at 295 K. At 295 K, there is no phase transition between α- and β-Si_3N_4, which is confirmed by our calculations.

It is generally accepted that the transition pressure of α to β phase occurs at elevated temperatures above 1500 K.[5,14] Thus, we calculate the pressure dependence of the Gibbs free energy to find out whether there exists a phase transition. In Fig. 4, we show the calculated Gibbs free energy difference G_α–G_β as a function of pressure at 1600 K. This figure shows that Si_3N_4 will undergo a structural phase transformation from α phase to β phase with pressure increasing. The intersection (G_α–$G_\beta = 0$) implies that the phase transition occurs at 7.98 GPa and 1600 K. α-Si_3N_4 has a lower Gibbs free energy at low pressure, and β-Si_3N_4 has a lower Gibbs free energy at pressures higher than 7.98 GPa, which indicates that at sufficiently high pressure β-Si_3N_4 would be favoured. The

calculated transition pressure is in excellent agreement with the result of 7.7 GPa (at 1573 K) using transmission electron microscopy from Danilenko *et al.*[14] in 1992. They found that the phase transition begins at 1573 K (The amount of β-Si_3N_4 increases with temperature increasing) and ends at 2373 K. Even in the initial stage, the perfect grains of the β-phase Si_3N_4 are formed. We think that the $\alpha \rightarrow \beta$ transformation is a solid-state reconstructive transition process, which will not occur below 1500 K. The reason why temperatures above 1500 K are required for the phase transition is that solvents suitable for the generation of β-Si_3N_4 do not melt until 1500 K–1700 K.[8]

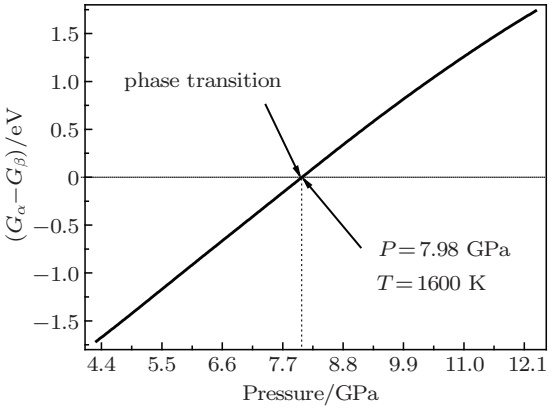


Fig. 4. Gibbs free energy difference G_α–G_β as a function of pressure.

3.3. Elastic and thermodynamic properties at finite temperature

In Figs. 5(a) and 5(c), we illustrate the normalized lattice parameters (a/a_0, c/c_0, V/V_0) for α- and β-Si_3N_4 at 0 K (obtained by the PW–PP method). a_0, c_0, and V_0 are the zero pressure equilibrium lattice parameters and cell volume, while a, c, and V represent the lattice parameters and cell volume at given pressures. In Figs. 5(b) and 5(d), the normalized volume V/V_0 dependences on pressure P at 0, 600, and 1500 K are plotted. It is obvious from Figs. 5(a) and 5(c) that, a/a_0 decreases faster than c/c_0 with a little difference. All the parameters smoothly decrease as pressure increases and no fluctuation can be seen. For α- and β-Si_3N_4, the c-axis crystal direction is substantial, slightly more incompressible than along a-axis direction, which is in agreement with the experimental measurements.[8,17,47] At 0 K and 10 GPa, the a/a_0 (α-Si_3N_4), c/c_0 (α-Si_3N_4), a/a_0 (β-Si_3N_4), and c/c_0 (β-Si_3N_4) values are 0.9857, 0.9867, 0.9863, and 0.9877, respectively. This result indicates that β-Si_3N_4 is more incompressible in the a and c axes than α-Si_3N_4. From Figs. 5(b) and 5(d), we can see that the temperature effects on Si_3N_4 are very small. As shown in Fig. 5(d), both the temperature effect and the pressure effect on V/V_0 are so small that β-Si_3N_4 is considered as an incompressible material. Besides, the values of zero temperature V/V_0 obtained from the PW–PP method and the QHD method accord well with each other.

Since pure single α- and β-Si_3N_4 crystals are hard to grow, very few experimental data are available on the elastic modulus of Si_3N_4. Using the QHD method, the pressure dependences of bulk moduli at three different temperatures are calculated and plotted in Fig. 6. It is clear in Fig. 6(a) that B increases with pressure increasing linearly and sharply at a given temperature, and at low temperature B is larger than at high temperature. The effect of pressure increasing on Si_3N_4 is the same as that of its temperature decreasing. Figure 6(b) shows the computed bulk moduli versus pressure at high temperatures, where the phase transition is also considered. As expected, B (α-Si_3N_4) increases monotonically with applied pressure up to 7 GPa. The bulk modulus undergoes a sudden upward jump at approximately 8 GPa, which is believed to be a first-order phase transition. When $P > 8$ GPa, the variation in bulk modulus with temperature is trivial. This indicates that the temperature effect on α-Si_3N_4 is greater than on β-Si_3N_4. The pressure effect on α-Si_3N_4 is similar to on β-Si_3N_4. Figure 6(c) is the pressure dependence of bulk modulus for β-Si_3N_4. Similar to Fig. 6(a), the relationship between bulk modulus and pressure is linear.

The calculated bulk moduli for α-Si_3N_4 are 234.9 GPa ($P = 0$, $T = 0$) and 233.3 GPa ($P = 0$, $T = 300$ K), which are in agreement with the theoretical values (228.5 GPa,[17] 257 GPa,[22] 242.5 GPa,[31] 229 GPa–248 GPa[17,48]) and the experimental data (256 GPa,[11] 223 GPa,[44] 248 GPa,[49] 282 GPa[50]). It is worth while noting that the experimental data are measured under ambient conditions and the theoretical values are usually obtained at 0 K. Although these values are widely scattered (maximal relative error reaches 27%), the agreement between our calculated results and the available data is excellent. For β-Si_3N_4, the bulk moduli obtained by the QHD method are 212.4, 221.7, 231.4, 241.5, 252.1, and 263.1 GPa at pressures of 0, 2, 4, 6, 8, and 10 GPa, respectively. The bulk moduli obtained by the PW–PP method are 237.3 ($P = 0$), 241.1 ($P = 2$ GPa), 247.6 ($P = 4$ GPa), 254.3 ($P = 6$ GPa), 261.2 ($P = 8$ GPa), and 266.8 GPa ($P = 10$ GPa). Good agreement is observed between *ab initio* bulk modulus and QHD bulk modulus.

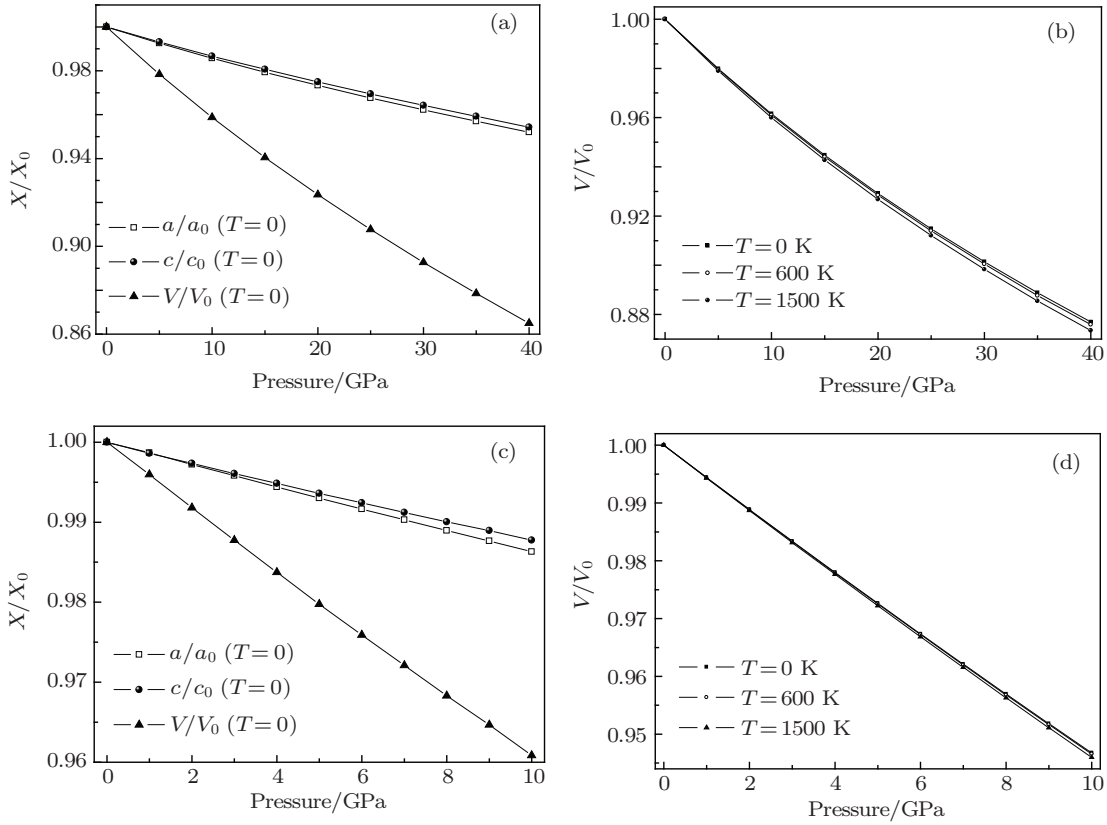


Fig. 5. Pressure dependences of normalized lattice parameters (a/a_0, c/c_0, V/V_0) for α-Si_3N_4 (a); V/V_0 obtained by the QHD model for α-Si_3N_4 (b); the same as (a), but for β-Si_3N_4 (c); the same as (b), but for β-Si_3N_4 (d).

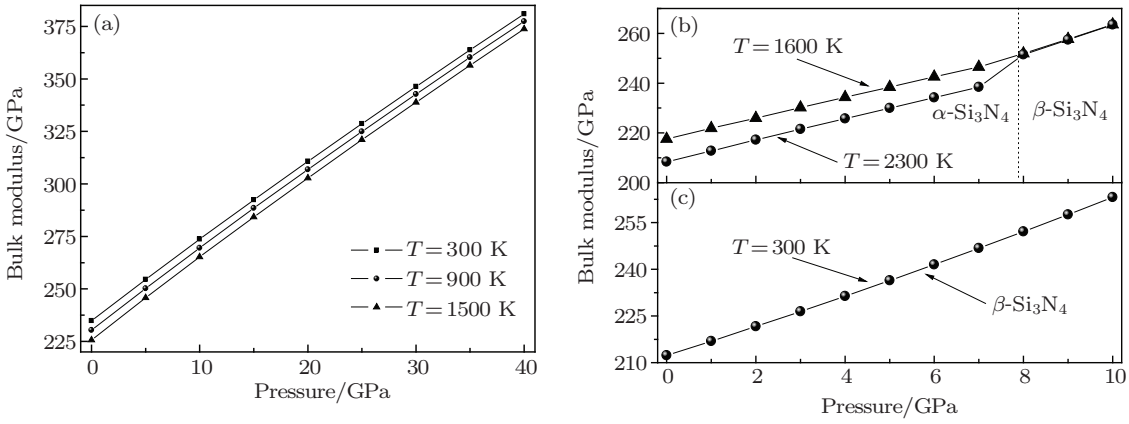


Fig. 6. Pressure dependences of the values of bulk modulus B in α-Si_3N_4 at different temperatures (a); pressure dependences of bulk modulus in α- and β-Si_3N_4 considering the phase transition (b); pressure dependence of B in β-Si_3N_4 at 300 K (c).

In Fig. 7(a), we present the variations of the entropy S each as a function of temperature for α-Si_3N_4. Several interesting features are revealed. At a given pressure, S increases sharply with temperature increasing up to 900 K. From this temperature, S approaches to an almost linear increase with temperature increasing. The propensity of increase becomes moderate, which means that the temperature dependence of S is moderate at high temperature. There exists two knee points (at 300 K and 900 K) when S changes with temperature increasing. The slope between S and T is significantly greater after the first knee point (at 300 K) than before the first knee point. After the second knee point (at 900 K), the relationship between S and T is opposite. At a given temperature, S decreases moderately with the increase of pressure. The increasing of S with temperature becomes smaller as pressure increases.

The temperature effect on S is more important than the pressure effect. At 0 GPa, our calculated entropies are 44.63 and 206.72 J·mol^{-1}·K^{-1} at 300 K and 1000 K, respectively. The entropies obtained by Wendel and Goddard *et al.*[8] are 55.53 (at 300 K) and 211.69 J·mol^{-1}·K^{-1} (at 1000 K). Data from the JANAF Thermochemical Tables[51] are 124.41 (at 300 K) and 270.64 J·mol^{-1}·K^{-1} (at 1000 K). The values derived from the Thermo-Properties of Individual Substances (TPIS)[52] are 72.29 (at 300 K) and 222.52 J·mol^{-1}·K^{-1} (at 1000 K). The wide range of the scattering can be ascribed mainly to the lack of single-crystal samples with good quality.[8] Another probable reason for this discrepancy is that the Si_3N_4 material might have strong anharmonicity at low temperature and pressure. Although these entropies are scattered, our calculated values are in reasonable agreement with them.

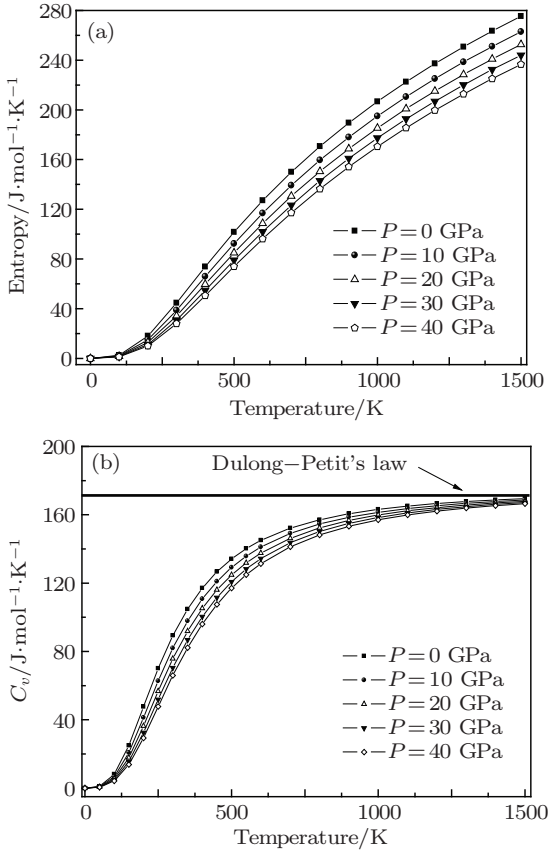


Fig. 7. Entropies (a) and heat capacities (b) versus temperature at different pressures for α-Si_3N_4.

The evolutions of the constant-volume heat capacities C_v for α-Si_3N_4 are drawn in Fig. 7(b). The temperature dependence of the heat capacity follows the Debye law. At sufficiently low temperature $C_v(T) \sim T^3$ and tends to zero when the temperature vanishes. At intermediate temperature, C_v is governed by the details of vibrations of different atoms and for a long time could only be determined from experimental measurements. C_v indicates a sharp increase up to 700 K, which is due to the anharmonic approximation of the QHD method used here. At high temperature, the anharmonic effect on C_v is suppressed and C_v is very close to the Dulong–Petit's classical limit ($3R$ for monoatomic material, 174 J·mol^{-1}·K^{-1} for α- and β-Si_3N_4). The heat capacity increases with temperature increasing at a given pressure, and decreases with applied pressure increasing at a constant temperature. It can also be seen from Fig. 7(b) that the temperature effect on C_v is greater than the pressure effect.

Applying the QHD method, the zero pressure heat capacities for α-Si_3N_4 are determined to be 8.13, 47.63, 89.91, 134.17, 152.18, 160.58, 165.08, 167.75, and 169.45 J·mol^{-1}·K^{-1} at temperatures of 100, 200, 300, 500, 700, 900, 1100, 1300, and 1500 K, respectively. The experimentally measured values of C_v at 300, 500, and 1100 K are 96.84, 127.94, and 165.21 J·mol^{-1}·K^{-1}, respectively.[53] Besides, Wendel and Goddard[8] have investigated the heat capacities of α- and β-Si_3N_4 using molecular dynamics simulation. Their calculated heat capacities for α-Si_3N_4 are 15.29 (T = 100 K), 52.61 (T = 200 K), 85.81 (T = 300 K), 127.33 (T = 500 K), 146.92 (T = 700 K), 156.81 (T = 900 K), 162.32 (T = 1100 K), 165.66 (T = 1300 K), and 167.82 J·mol^{-1}·K^{-1} (T = 1500 K). Our calculated heat capacities are in excellent agreement with the experimental data and previous theoretical results. Unfortunately, at high pressures there are no results available to compare with our data.

The values of entropy S and the heat capacity C_v of β-Si_3N_4 are listed in Table 1, together with available experimental values and theoretical results. It is noticed that at a fixed pressure P, S and C_v increase exponentially with temperature T, and then their increases trend gentler. The effects of temperature on S and C_v are more significant than the effects of pressure, especially at low temperature. S and C_v display roughly similar behaviors in the whole temperature range of 0–2300 K. For α-Si_3N_4, the JANAF data[51] differs significantly from those of TPIS[52] and Ref. [8]. Our results are in agreement with the TPIS data and the values listed in Ref. [8]. Our computed S and C_v are in agreement with the theoretical results obtained by Wendel and Goddard[8] and the values given in Refs. [51] and [52]. The maximal absolute errors be-

tween our results and the results shown in Ref. [8] for entropy S (β-Si_3N_4), heat capacity C_v (β-Si_3N_4), and entropy S (α-Si_3N_4) are 8.90 (at 300 K), 11.32 (at 200 K), and 10.90 J·mol^{-1}·K^{-1} (at 300 K), respectively. The agreement between our results and the results given in the other work partially proves the validity of the QHD method at high temperatures. It is important to notice that the neglect of intrinsic anharmonicity in the quasi-harmonic approximation leads to an overestimation of entropy at low temperature and low pressure. On the other hand, the experimental measurements of S and C_v are taken from polycrystalline samples including porosities and defects. However, in our calculation all thermodynamic properties are related to ideal crystal.

Table 1. Values of entropy S and heat capacity C_v of Si_3N_4. All functions are calculated per Si_3N_4 formula unit to facilitate comparisons between the α- and β-phases. The available experimental and theoretical data are also reported.

	S/J·mol^{-1}·K^{-1} (β-Si_3N_4)				C_v/J·mol^{-1}·K^{-1} (β-Si_3N_4)				S/J·mol^{-1}·K^{-1} (α-Si_3N_4)			
P	0	0	4	7.7	0	0	4	7.7	0	0	0	0
T/K	Ref. [8]	Calc.	Calc.	Calc.	Ref. [8]	Calc.	Calc.	Calc.	Calc.	Ref. [8]	JANAF[51]	TPIS[52]
100	5.93	2.76	2.70	2.64	15.59	6.68	6.53	6.39	2.53	5.78	–	–
200	28.09	19.33	18.96	18.62	52.91	41.59	40.91	40.29	17.99	27.70	–	44.17
300	56.03	47.12	46.42	45.78	85.79	82.25	81.42	80.66	44.63	55.53	124.41	72.29
400	84.25	77.02	76.10	75.26	110.19	110.97	110.25	109.59	73.84	83.83	152.49	105.21
500	110.77	105.18	104.12	103.16	127.08	129.34	128.76	128.23	101.65	110.40	180.62	128.50
600	135.03	130.70	129.55	128.51	138.66	141.19	140.74	140.32	127.03	134.71	200.55	150.99
700	157.05	153.65	152.44	151.35	146.71	149.11	148.74	148.41	149.96	156.76	217.58	170.28
800	177.03	174.32	173.07	171.94	152.45	154.58	154.29	154.02	170.70	176.77	236.04	188.77
900	195.25	193.04	191.77	190.61	156.65	158.51	158.26	158.04	189.50	195.00	254.54	206.45
1000	211.92	210.11	208.81	207.64	159.79	161.40	161.20	161.01	206.72	211.69	270.64	222.52
1100	227.27	225.77	224.45	223.26	162.20	163.59	163.42	163.26	222.55	227.05	287.48	237.80
1200	241.46	240.21	238.88	237.67	164.07	165.28	165.14	165.01	237.18	241.26	301.86	250.67
1300	254.66	253.60	252.26	251.04	165.56	166.62	166.49	166.38	250.77	254.46	314.06	261.93
1400	266.97	266.08	264.73	263.50	166.77	167.69	167.58	167.48	263.47	266.78	326.96	277.20
1500	278.51	277.76	276.40	275.17	167.75	168.56	168.46	168.38	275.36	278.33	338.97	289.28
1600	289.37	288.73	287.36	286.12	168.56	169.28	169.19	169.11	–	289.18	348.64	299.74
1700	299.61	299.07	297.69	296.45	169.24	169.87	169.80	169.73	–	299.43	360.73	310.21
1800	309.30	308.84	307.47	306.22	169.81	170.38	170.31	170.25	–	309.12	371.19	320.67
1900	318.49	318.12	316.73	315.48	170.30	170.80	170.74	170.69	–	318.32	380.85	331.14
2000	327.24	326.93	325.54	324.29	170.71	171.17	171.12	171.06	–	327.07	390.52	340.80
2100	335.57	335.33	333.94	332.68	171.07	171.49	171.44	171.39	–	335.41	399.38	349.67
2200	343.54	343.35	341.96	340.70	171.39	171.76	171.72	171.67	–	343.37	409.85	359.33
2300	351.17	351.03	349.63	348.37	171.66	172.00	171.96	171.92	–	351.00	416.54	367.36

The Debye temperature θ_D is one of the most important thermodynamic parameters of solids. When $T < \theta_D$, quantum mechanical effects are very important for clarifying the thermodynamic properties of materials, while $T > \theta_D$ quantum effects can be ignored. The calculated Debye temperatures of the Si_3N_4 polymorphs are shown in Table 2. Our results regarding α-Si_3N_4 listed in Table 2 are predictions, since no experimental and theoretical data are available for α-Si_3N_4. We observe that all Debye temperatures decrease monotonically and almost linearly with temperature increasing. The Debye temperature θ_D of Si_3N_4 has roughly the same pressure dependence, showing an increase of the Debye temperature with pressure increasing. At the same temperature and pressure, θ_D for α-Si_3N_4 is greater than the Debye temperature for β-Si_3N_4. This is in agreement with our bulk modulus analysis because, as is well known, the Debye temperature is proportional to the bulk modulus and that hard materials usually exhibit elevated Debye temperatures. At 0 GPa, θ_D drops by less than 1.61% and 0.13% (between 0 and 1500 K) for α- and β-Si_3N_4, respectively. The temperature effect is very small since θ_D is still above 1150 K at high temperatures. The experimentally determined values of θ_D for β-Si_3N_4 are 1100 K (at 300 K)[54] and 1160 K

(at 0 K)[55] and 1140 K (at high temperatures).[55] The theoretical values are 1140 K[56] and 1050 K–1100 K.[56] The agreement between our results and these values are excellent.

Table 2. Values of Debye temperature $\theta_{\rm D}$ (K) of α- and β-Si_3N_4 at different temperatures and pressures.

	α-Si_3N_4			β-Si_3N_4		
T/K	0/GPa	15/GPa	30/GPa	0/GPa	5/GPa	10/GPa
0	1178.08	1303.24	1408.54	1159.65	1171.15	1182.53
300	1177.14	1302.61	1408.08	1159.57	1171.09	1182.48
600	1173.57	1300.22	1405.94	1159.29	1170.84	1182.26
900	1169.40	1296.64	1403.05	1158.92	1170.52	1181.97
1200	1164.44	1292.79	1399.89	1158.53	1170.18	1181.66
1500	1159.34	1288.80	1396.60	1158.12	1169.82	1181.34

4. Conclusion

In this paper, we present complete investigations for the structural, elastic, thermodynamic properties, and the phase transition characters of α- and β-Si_3N_4 by using the plane-wave pseudo-potential method in combination with the Debye-like (QHD) model. The predicted lattice parameters of α-Si_3N_4 are given. Full geometry optimization of β-Si_3N_4 is carried out to obtain the fundamental properties like lattice parameters, cell volumes, elastic constants, elastic moduli, Poisson ratios, and compressibilities of β-Si_3N_4. Our results can be summarized as follows.

(i) The investigation shows that β-Si_3N_4 is a mechanically stable material in a pressure range of 0–10 GPa. β-Si_3N_4 is a hard material with very small compressibility and relatively high bulk modulus, which also exhibits a ductile behaviour. Besides, the high-pressure nature of the chemical bonding in β-Si_3N_4 is dominated by the presence of ionic character.

(ii) Calculations show that the α → β phase transition cannot be observed in a temperature range of 0–300 K and a pressure range of 0–40 GPa. The β-type Si_3N_4 is more energy favourable than α-Si_3N_4. Additionally, the transition pressure is found to be 7.98 GPa at 1600 K.

(iii) Both the pressure dependence and the temperature dependence of bulk moduli B, lattice parameters a/a_0, c/c_0, and cell volumes V/V_0 are analysed. For the two polymorphs, the c axes are less compressible than the a axes. The *ab initio* bulk moduli and the QHD bulk moduli are in agreement with each other.

(iv) Through the QHD model, the dependences of the bulk modulus B, entropy S, heat capacity C_v, and Debye temperature $\theta_{\rm D}$ on temperature and pressure are successfully obtained. C_v is found to increase with temperature increasing and is close to the Dulong–Petit's limit at high temperature. S increases sharply with temperature increasing first, and then the propensity of increase becomes moderate. The temperature effects on S and C_v are significant while the pressure effects on B and $\theta_{\rm D}$ are important.

Our calculated results are well consistent with available experimental data and previous theoretical results. Our calculations may provide useful information for theoretical and experimental researches on Si_3N_4 polymorphs, but still await experimental confirmation.

Acknowledgment

The authors are grateful to Prof. M. A. Blanco and his colleagues for their GIBBS calculation code, and also to Prof. P. Giannozzi and his co-workers for the QUANTUM ESPRESSO package.

References

[1] Yang H S, Nie A M and Qiu F M 2010 *Chin. Phys.* B **19** 017202
[2] Xu B, Dong J, McMillan P, Shebanova O and Salamat A 2011 *Phys. Rev.* B **84** 014113
[3] Chen J, Ouyang L Z, Rulis P, Misra A and Ching W Y 2005 *Phys. Rev. Lett.* **95** 256103
[4] Zerr A, Miehe G, Serghiou G, Schwarz M, Kroke E, Riedel R, Fuess H, Kroll P and Boehler R 1999 *Nature* **400** 340
[5] Wang L G, Sun J X, Yang W and Tian R G 2008 *Acta Phys. Pol.* A **114** 807
[6] Chen L W and Chen C H 1994 *Chin. Phys. Lett.* **11** 281
[7] Kuwabara A, Matsunaga K and Tanaka I 2008 *Phys. Rev.* B **78** 064104
[8] Wendel J A and Goddard III W A 1992 *J. Chem. Phys.* **97** 5048
[9] Ching W Y, Xu Y N, Gale J D and Rühle M 1998 *J. Am. Ceram. Soc.* **81** 3189
[10] Dodd S P, Cankurtaran M, Saunders G A and James B 2001 *J. Mater. Sci.* **36** 2557
[11] Yashima M, Ando Y and Tabira Y 2007 *J. Phys. Chem.* B **111** 3609
[12] Chen J F, Ren Z X and Ding Z F 1995 *Acta Phys. Sin. (Overseas Edn.)* **4** 698
[13] Zhang C, Sun J X, Tian R G and Zou S Y 2007 *Acta Phys. Sin.* **56** 5969 (in Chinese)
[14] Danilenko N V, Oleinik G S, Dobrovol'skii V D, Britun V F and Semenenko N P 1992 *Powder Metal. Met. Ceram.* **31** 1035
[15] Butler I S and Huang Y 1992 *Appl. Spectrosc.* **46** 1303
[16] Togo A and Kroll P 2008 *NIC Symposium* **39** 95
[17] Kruger M B, Nguyen J H, Li Y M, Caldwell W A, Manghnani M H and Jeanloz R 1997 *Phys. Rev.* B **55** 3456

[18] Mirgorodsky A P, Baraton M I and Quintard P 1993 *Phys. Rev.* B **48** 13326
[19] Meléndez-Martínez J J and Domínguez-Rodríguez A 2004 *Prog. Mater. Sci.* **49** 19
[20] Bermudez V M 2005 *Surf. Sci.* **579** 11
[21] Belkada R, Kohyama M, Shibayanagi T and Naka M 2002 *Phys. Rev.* B **65** 092104
[22] Ching W Y, Ouyang L Z and Gale J D 2000 *Phys. Rev.* B **61** 8696
[23] Weiss J 1981 *Ann. Rev. Mater. Sci.* **11** 381
[24] Grün R 1979 *Acta Cryst.* B **35** 800
[25] Kohn W and Sham L J 1965 *Phys. Rev.* **140** A1133
[26] Giannozzi P, Baroni S and Bonini N 2009 *J. Phys.: Condens. Matter* **21** 395502
[27] Perdew J P, Burke K and Ernzerhof M 1996 *Phys. Rev. Lett.* **77** 3865
[28] Monkhorst H J and Pack J D 1976 *Phys. Rev.* B **13** 5188
[29] Blanco M A, Francisco E and Luaña V 2004 *Comput. Phys. Commun.* **158** 57
[30] Murnaghan F D 1944 *Proc. Natl. Acad. Sci. USA* **30** 238
[31] Marian C M, Gastreich M and Gale J D 2000 *Phys. Rev.* B **62** 3117
[32] Hirosaki N, Ogata S, Kocer C, Kitagawa H and Nakamura Y 2002 *Phys. Rev.* B **65** 134110
[33] Borgen O and Seip H M 1961 *Acta Chem. Scand.* **15** 1789
[34] Priest H F, Burns F C, Priest G L and Skaar E C 1973 *J. Am. Ceram. Soc.* **56** 395
[35] Jiang C, Lin Z and Zhao Y 2009 *Phys. Rev. Lett.* **103** 185501
[36] Pugh S F 1954 *Philos. Mag.* **45** 823
[37] Han I S, Seo D W, Kim S Y, Hong K S, Guahk K H and Lee K S 2008 *J. Eur. Ceram. Soc.* **28** 1057
[38] Shein I R and Ivanovskii A I 2008 *Scr. Mater.* **59** 1099
[39] Haines J, Léger J M and Bocquillon G 2001 *Ann. Rev. Mater. Res.* **31** 1
[40] Wang H, Chen Y, Kaneta Y and Iwata S 2006 *J. Phys.: Condens. Matter* **18** 10663
[41] Wang A J, Shang S L, Du Y, Kong Y, Zhang L J, Chen L, Zhao D D and Liu Z K 2010 *Comput. Mater. Sci.* **48** 705
[42] Watari K 2001 *J. Ceram. Soc. Jpn.* **109** S7
[43] Vogelgesang R, Grimsditch M and Wallace J S 2000 *Appl. Phys. Lett.* **76** 982
[44] Zerr A, Kempf M, Schwarz M, Kroke E, Göken M and Riedel R 2002 *J. Am. Ceram. Soc.* **85** 86
[45] Shebanova O, Soignard E and Mcmillan P F 2006 *High Pres. Res.* **26** 87
[46] Kroll P, Milko M and Anorg Z 2003 *Allg. Chem.* **629** 1737
[47] Cartz L and Jorgensen J D 1981 *J. Appl. Phys.* **52** 236
[48] Yeheskel O and Gefen Y 1985 *Mater. Sci. Eng.* **71** 95
[49] Yeheskel O, Gefen Y and Talianker M 1986 *Mater. Sci. Eng.* **78** 209
[50] Srinivasa S R, Cartz L, Jorgensen J D, Worlton T G, Beyerlein R A and Billy M 1977 *J. Appl. Crystallogr.* **10** 167
[51] Chase M W, Davies C A, Downey J R, Frurip D J, McDonald R A and Syverad A N 1985 *JANAF Thermochemical Tables* (New York: American Chemical Society Press)
[52] Gurvich L V, Veyts I V and Alcock C B 1989 *Thermodynamic Properties of Individual Substances* (New York: Hemisphere Press)
[53] Loong C K, Vashishta P, Kalia R K and Ebbsjö I 1995 *Europhys. Lett.* **31** 201
[54] Watari K, Seki Y and Ishizaki K 1989 *J. Ceram. Soc. Jpn. Inter. Ed.* **97** 174
[55] Slcak G A and Huseby I C 1982 *J. Appl. Phys.* **53** 6817
[56] Schwarz M R 2003 *High Pressure Synthesis of Novel Hard Materials: Spinel*-Si_3N_4 *and Derivates* (Kassel: Kassel University Press)